Supporting Information

Highly Active, CO-Tolerant and Robust Hydrogen Anode Catalysts: Pt-M (M = Fe, Co, and Ni) Alloys with Stabilized Pt Skin Layers

Guoyu Shi,[a] Hiroshi Yano,[b] Donald A. Tryk,[b] Akihiro Iiyama,[b] and Hiroyuki Uchida[b, c]*

[a]*Interdisciplinary Graduate School of Medicine and Engineering, University of Yamanashi, Takeda 4, Kofu, 400 8510, Japan*
[b]*Fuel Cell Nanomaterials Center, University of Yamanashi, Takeda 4, Kofu, 400-8510, Japan*
[c]*Clean Energy Research Center, University of Yamanashi, Takeda 4, Kofu, 400-8510, Japan*
E-mail: h-uchida@yamanashi.ac.jp; Fax: +81-55-220-8618; Tel: +81-55-220-8619

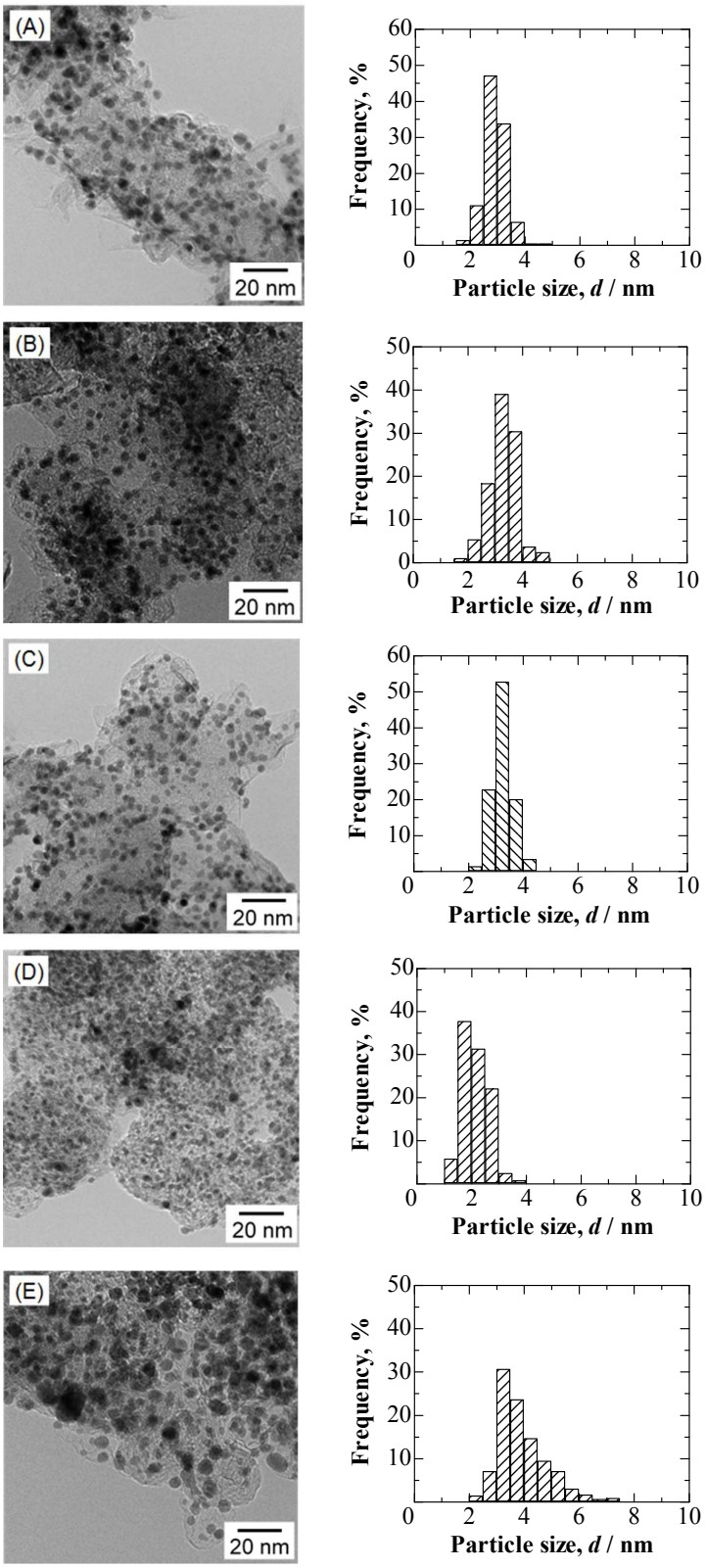

Figure S1. TEM images and particle size distribution histograms of (A) Pt_{2AL}–PtFe/C, (B) Pt_{2AL}–PtCo/C, (C) Pt_{2AL}–PtNi/C, (D) c-Pt/C and (E) c-Pt_2Ru_3/C catalysts.

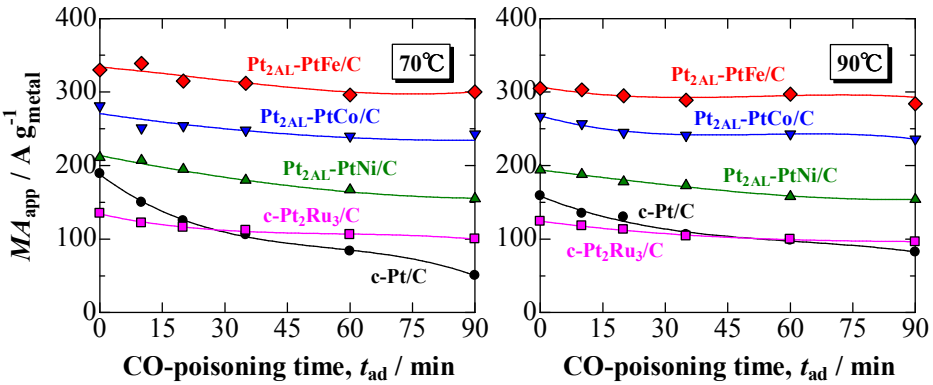

Figure S2. Change in the MA_{app} with CO-poisoning time (t_{ad}) for Pt_{2AL}–PtFe/C, Pt_{2AL}–PtCo/C, Pt_{2AL}–PtNi/C, c-Pt/C and c-Pt_2Ru_3/C at 70°C and 90°C. After each electrode was exposed to 0.1 M $HClO_4$ solution saturated with 1000 ppm CO (H_2-balance) at 0.05 V for a given period t_{ad}, the MA_{app} was evaluated in H_2-saturated 0.1 M $HClO_4$ solution.

DFT Calculation Details

In order to obtain reliable estimates of adsorption energies for carbon monoxide and atomic hydrogen, we have used high-accuracy electronic structure density function theoretical (DFT) calculations, taking into account relativistic effects. In the present work, we have carried out the DFT calculations with the DMol^3 software package (BIOVIA, Materials Studio, Version 7.0).[S1] The finest settings were used for the geometric optimization (convergence criteria, 1×10^{-5} Ha, maximum force 0.002 Ha/Å, maximum displacement 0.005 Å), which was carried out with density functional semicore pseudopotentials,[S2] with a double-numeric quality basis set with polarization functions (dnp), and the final energies were calculated with all-electron scalar relativistic corrections. The gradient-corrected GGA functional used was developed by Perdew, Burke and Ernzerhof (pbe).[S3] To facilitate scf convergence, kinetic energy was applied to the electrons (thermal smearing) of 0.005 Ha for Pt(110) and 0.003 Ha for the Pt-Co alloys.

Periodic boundary conditions (PBC) were used for the (221) surfaces for pure Pt and the four alloy systems, Pt-Fe, Pt-Co Pt-Ni, and Pt-Ru, with three layers of metal atoms (Pt and/or Fe, Co, Ni or Ru), which consisted of steps and 3-atom-wide terraces, with a surface mesh of 2×4, as shown as a side view in Figure S3. For the alloy systems, half of the atoms in the top layer were converted from Fe, Co, Fe or Ru to Pt to simulate the formation of a Pt skin layer. To simulate the Pt_{1AL}–PtFe(221), Pt_{1AL}–PtCo(221), Pt_{1AL}–PtNi(221) and Pt_{1AL}–PtRu(221) surfaces, with their higher concentrations of Fe, Co, Ni or Ru close to the surface, half of the atoms in the second layer were converted from Pt to Fe, Co, Ni or Ru.

For pure Pt, the lattice parameter used for the face-centered cubic (fcc) structure was the standard experimental bulk value of 3.93 Å; for Pt_3Ni, the fcc lattice parameter was 3.844 Å (space group Pm-3m),[S4] for Pt_3Co, the fcc lattice parameter was 3.831Å (space group Pm-3m),[S5] for Pt_3Fe, the fcc lattice parameter was 3.87 Å (space group Pm-3m).[S6] For Pt_3Ru, the lattice parameter was calculated to be 3.8845 Å, based on Vegard's Law and the bulk composition (Pt_2Ru_3). For all of these structures, the xyz coordinates of the 8 bottom layer atoms were constrained to conform to those of the bulk structure. Together with the present results, various representative results from the literature are shown for both calculated and experimental adsorption energies for CO, H, and H_2 on Pt(111), as a reference for (221) terraces, Pt(110), as a reference for (221) steps, and Pt-M(111) surfaces in Table S1. In the present work, the results were calculated for the cases depicted in Figure S3 and Figure 3 in the main text, i.e., undissociated H_2 at 1/8 ML coverage, 2H at 1/8 ML coverage at steps and 1/4 ML coverage on terraces, CO at 1/8 ML coverage on both steps and terraces, and H_2O at 1/8 ML coverage on both steps and terraces. The experimental values are given for both low and high coverages. In general, the DFT results tend to overestimate the adsorption strengths, and the adsorption strengths on the (111) surfaces are smaller than those on the (110) surfaces.

It should be noted that the value obtained for the pure Pt(111) terrace, -1.74 eV, is somewhat weaker than that obtained by Orita for the flat Pt(111) surface, -1.94 eV, using similar methods,[S18] which was at the edge of the experimental range of -1.90 to -1.64 eV obtained experimentally.[S14]

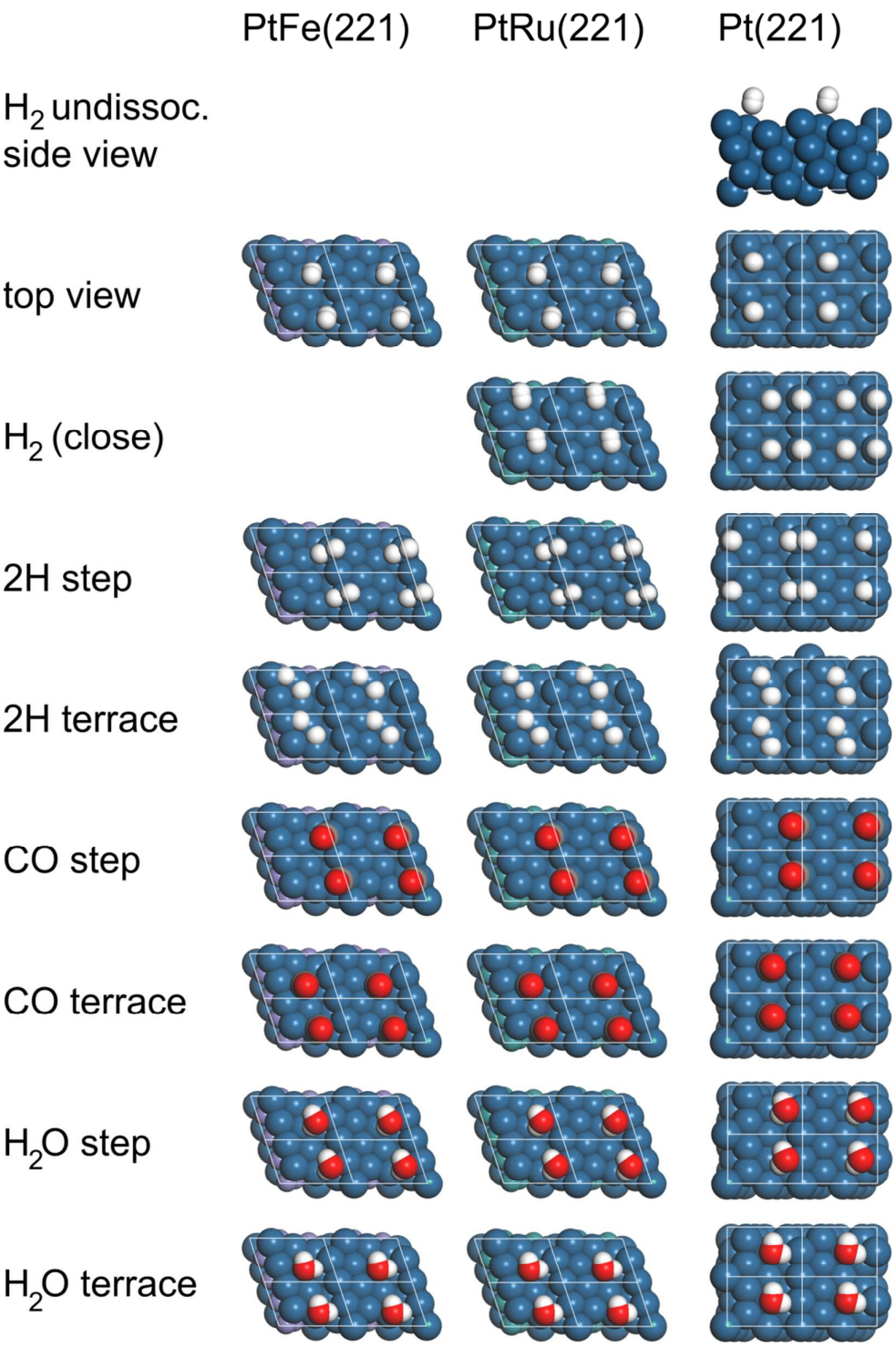

Figure S3. Top views of models used for DFT calculations with (left) Pt_{1AL}–PtFe(221) (as a representative for Pt_{1AL}–PtCo(221) and Pt_{1AL}–PtNi(221), since the adsorption configurations were identical for all three), (middle) Pt_{1AL}–PtRu(221), and (right) Pt(221), for the adsorption of (top to bottom) H_2 (undissociated, side view; undissociated, top view; undissociated close contact, top view, for PtRu and Pt only), 2H(step; terrace), CO(step; terrace) and H_2O(step; terrace). Four surface unit cells are shown in each case in order to better observe the periodicity of the model and adsorption.

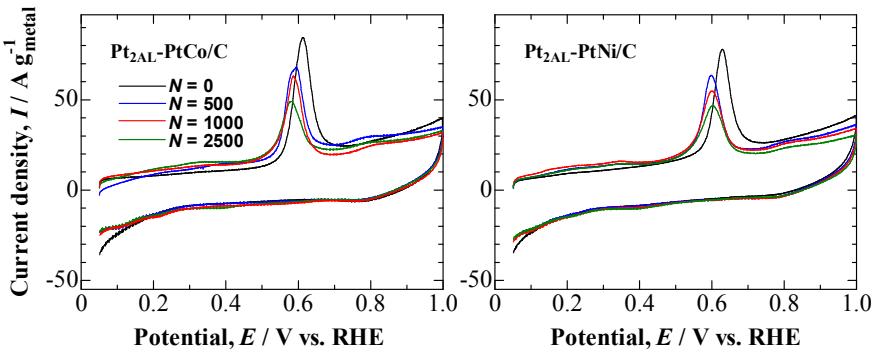

Figure S4. CO stripping voltammograms at Nafion-coated Pt_{2AL}–PtCo/C and Pt_{2AL}–PtNi/C electrodes at a given potential cycle number of *N* measured in N_2-saturated 0.1 M $HClO_4$ solution at 70°C and potential sweep rate of 20 mV s^{-1}.

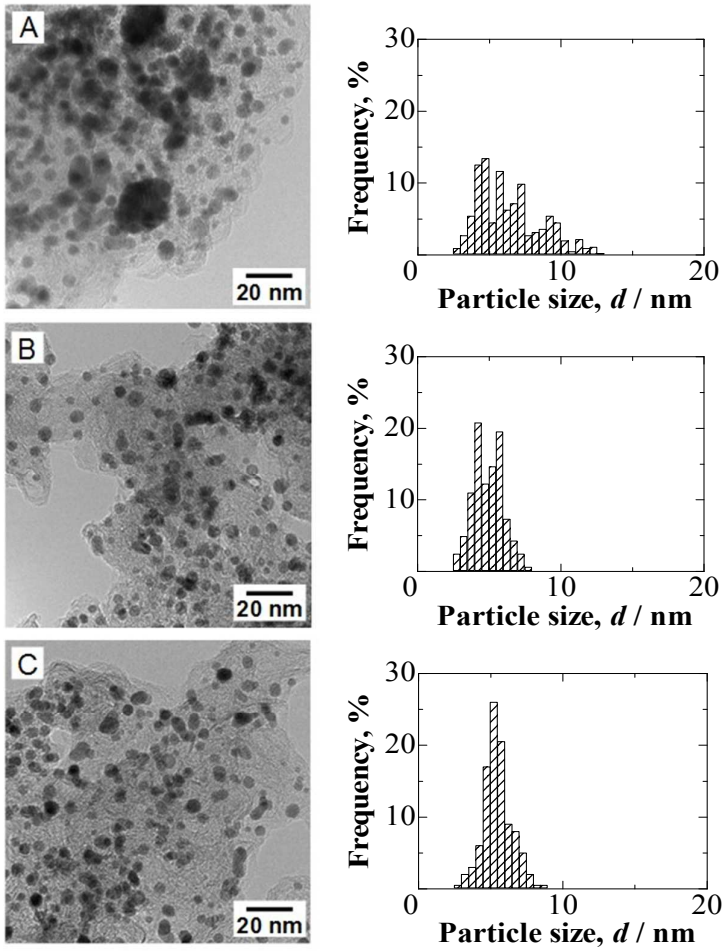

Figure S5. TEM images and particle size distribution histograms of (A) c-Pt/C, (B) Pt_{2AL}–PtCo/C, and (C) Pt_{2AL}–PtNi/C after the durability test at $N = 2500$.

Table S1. Adsorption energies for CO, H and H_2 and H_2 dissociation energies on various Pt and Pt-M alloy surfaces; values are in eV (kJ mol^{-1}).

Surface	**CO on-top** [a]	**H** [b]	**H_2 float**[c]	**H_2 dissoc.**[d]
Pt(111) [e]	−1.83 (−176.6)[f]	−0.96 (−92.9)[g]		
Pt(111)[h]	−1.47 (−141.8)			
Pt(111)[j]	−1.61 (−155.3)			
Pt(221)-terrace[o]		−0.91 (−88.2)	−0.02 (−1.8)	−1.43 (−138.0)
Pt(111)(exp., low θ)[j]	−1.90 (−183.3)			
Pt(111)(exp., high θ)[j]	−1.66 (−160.2)			
Pt(111)[k]		−0.97 (−93.9)[k]		
Pt(111)(exp., low θ)[l]		−0.81 (−78.0)[l]		
Pt(111)(exp., high θ)[l]		−0.44 (−42.0)[l]		
Pt(221)-step[o]	−2.40 (−231.2)	−1.37 (−132.3)		−1.43 (−138.0)
Pt(110)(exp. , low θ)	−1.90 (−183.3)[n]	−1.12(−108.0)[o]		
Pt(110)(exp. , high θ)	−1.51 (−145.7)[n]	−0.77 (−74.0) [o]		
Pt-Ru(111) NSA[e]	−1.53 (−147.6) [f]	−0.58 (−56.2)[g]		
Pt-Ru(111)[i]	−1.08 (−104.2)			
Pt_{1AL}-PtRu(221)-step[m]	−2.18 (−210.6)	−1.09 (−105.0)		
Pt_{1AL}-PtRu(221)-terr[m]	−1.54 (−148.8)	−0.45 (−43.1)	−0.03 (−2.7)	−0.15 (−14.6)
Pt-Ni(111) NSA[e]	−1.20 (−115.8)	−0.60 (−58.1)[g]		
Pt/Pt_3Ni(111)[h]	−1.20 (−115.8)			
Pt_{1AL}-PtNi(221)-step[m]	−2.01 (−193.9)	−1.02 (−98.7)		
Pt_{1AL}-PtNi(221)-terr[m]	−1.20 (−115.5)	−0.17 (−16.5)	−0.02 (−2.0)	
Pt-Co(111) NSA[e]		−0.38 (−36.9)[g]		
Pt/Pt_3Co(111)[h]	−1.15 (−111.0)			
Pt_{1AL}-PtCo(221)-step[m]	−1.83 (−176.9)	−1.01 (−97.6)		
Pt_{1AL}-PtCo(221)-terr[m]	−1.04 (−100.7)	−0.07 (−6.8)	−0.03 (−3.3)	
Pt-Fe(111) NSA[e]	−1.11 (−107.1) [f]	−0.22 (−21.5)[g]		
Pt/Pt_3Fe(111)[h]	−1.13 (−109.0)			
Pt_{1AL}-PtFe(221)-step[m]	−1.89 (−182.5)	−0.99 (−95.2)		
Pt_{1AL}-PtFe(221)-terr[m]	−1.01 (−97.3)	+0.08 (+7.3)	−0.02 (−2.1)	

[a] The on-top configuration for CO is the most stable experimentally on both the Pt(111) and Pt(110) surfaces; on-top values were taken even if they were not calculated to be the most stable in Refs. S7 and S8.

[b] Referred to ½ H_2. Ref. S9 uses a gas-phase H atom as the reference; the values were converted here by subtracting ½ of the dissociation energy at 0 K (432.00 kJ mol^{-1})(Ref. S10). Binding sites are not distinguished on Pt(111) except for work of Ishikawa, for which the bridging site is used (Refs. S11, S12).

[c] Molecular H_2 adsorption does not occur experimentally under most conditions on pure Pt(111) or Pt(110); however, molecular ~~H_2~~ adsorption has ~~also~~ been considered for the pure Pt and alloy surfaces in the present work; for all alloys except PtRu, H_2 placed close to the terrace surface spontaneously "floated" ca. 1 A away from the surface; on Pt and PtRu, H_2 was also stable when

placed initially in a "floating" configuration; in an adsorbed state, it was stable only on the PtRu(221) terrace (see note d).

[d]The value given for PtRu(221) is actually for molecular H_2 adsorbed on the terrace. For pure Pt(221), H_2 placed close to the terrace surface spontaneously dissociates into one H adsorbed at the step and one on the terrace.

[e] Refs. S7 and S9 report DFT calculations for Pt(111) and related near-surface alloys, in which there is a layer of pure M below a Pt(111) monolayer surface.

[f] Ref. S7.

[g] Ref. S9, referred to gas-phase H atoms.

[h] Pt(111) or Pt(111) monolayer on Pt_3M alloy, Ref. S8.

[i] Pt(111) or Pt monolayer on Ru(0001), Ref. S13.

[j] Exp., 0.17-0.33 ML, Ref. S14.

[k] Ref. S11.

[l] Ref. S15.

[m] Present work.

[n] Ref. S16.

[o] Ref. S17.

Table S2. Average composition of the catalysts particles before ($N = 0$) and after durability test ($N = 2500$).

Catalyst	$N = 0$ [a)]		$N = 2500$ [b)]	
	Pt (atom %)	M (atom %)	Pt (atom %)	M (atom %)
Pt_{2AL}−PtFe/C	73.1	26.9	78.7	21.3
Pt_{2AL}−PtCo/C	67.2	32.8	69.3	30.7
Pt_{2AL}−PtNi/C	71.0	29.0	75.8	24.2
c-Pt_2Ru_3/C	40.4	59.6	50.9	49.1

a) Analyzed by ICP.
b) Analyzed by spot-analysis with EDX at 20 randomly selected particles.

References

(S1) Delley, B. *Int. J. Quant. Chem*. **1998**, *69*, 423-433.

(S2) Delley, B. *Phys. Rev. B* **2002**, *66*, 155125.

(S3) Perdew, J. P.; Burke, K.; Ernzerhof, M. *Phys. Rev. Lett.* **1996**, *77*, 3865.

(S4) Engelke, M. J. Local Atomic Arrangements in Ni-Pt: The Bulk and Near-Surface Regimes, Doctoral Dissertation (ETH-19104), ETH Zurich, 2010, p 29.

(S5) Geisler, A. H.; Martin, D. L. *J. Appl. Phys*. **1952**, *23*, 375.

(S6) Stamm, W.; Wassermann, E. F. *J. Magn. Magn. Mater*. **1986**, *54-57*, 161-162.

(S7) Greeley, J.; Mavrikakis, M. *Catal. Today* **2006**, *111*, 52-58.

(S8) van der Vliet, D. F.; Wang, C.; Li, D.; Paulikas, A. P.; Greeley, J.; Rankin, R. B.; Strmcnik, D.; Tripkovic, D.; Markovic, N. M.; Stamenkovic, V. R. *Angew. Chem. Int. Ed*. **2012**, *51*, 3139-3142.

(S9) Greeley, J.; Mavrikakis, M. *J. Phys. Chem. B* **2005**, *109*, 3460-3471.

(S10) Darwent, B. D. Bond Dissociation Energies in Simple Molecules, Nat. Stand. Ref. Data Ser., Nat. Bur. Stand. (U.S.) 31 (Jan. 1970) (http://www.nist.gov/data/nsrds/NSRDS-NBS31.pdf)

(S11) Ishikawa, Y.; Mateo, J. J.; Tryk, D. A.; Cabrera, C. R. *J. Electroanal. Chem.* **2007**, *607*, 37-46.

(S12) Mateo, J. J.; Tryk, D. A.; Cabrera, C. R.; Ishikawa, Y. *Mol. Simul*. **2008**, *34*, 1065-1072.

(S13) Koper, M. T. M.; Shubina, Y. E.; van Santen, R. A. *J. Phys. Chem. B* **2002**, *106*, 686-692.

(S14) Yeo, Y. Y.; Vattuone, L.; King, D. A. *J. Chem. Phys.* **1997**, *106*, 392-401.

(S15) Christmann, K. *Surf. Sci. Rep.* **1988**, *9*, 1-163.

(S16) Wartanby, C. E.; Stuck, A.; Yeo, Y. Y.; King, D. A. *J. Phys. Chem.* **1996**, *100*, 12483-12488.

(S17) Lipkowski, J.; Ross, P. N. *Electrocatalysis*, Wiley-VCH, New York, 1998.

(S18) Orita, H.; Itoh, N.; Inada, Y. *Chem. Phys. Lett.* **2004**, *384*, 271-276.